

In situ measurements of background aerosol and subvisible cirrus in the tropical tropopause region

Andreas Thomas,¹ Stephan Borrmann,^{1,2} Christoph Kiemle,³ Francesco Cairo,⁴ Michael Volk,⁵ Jürgen Beuermann,⁶ Boris Lepuchov,⁷ Vincenzo Santacesaria,⁸ Renaud Matthey,⁹ Vladimir Rudakov,¹⁰ Vladimir Yushkov,¹⁰ A. Robert MacKenzie,¹¹ and Leopoldo Stefanutti⁸

Received 12 October 2001; revised 3 July 2002; accepted 22 July 2002; published 19 December 2002.

[1] In situ aerosol measurements were performed in the Indian Ocean Intertropical Convergence Zone (ITCZ) region during the Airborne Polar Experiment-Third European Stratospheric Experiment on Ozone (APE-THESEO) field campaign based in Mahé, Seychelles between 24 February and 6 March 1999. These are measurements of particle size distributions with a laser optical particle counter of the Forward Scattering Spectrometer Probe (FSSP)-300 type operated on the Russian M-55 high-altitude research aircraft Geophysica in the tropical upper troposphere and lower stratosphere up to altitudes of 21 km. On 24 and 27 February 1999, ultrathin layers of cirrus clouds were penetrated by Geophysica directly beneath the tropical tropopause at 17 km pressure altitude and temperatures below 190 K. These layers also were concurrently observed by the Ozone Lidar Experiment (OLEX) lidar operating on the lower-flying German DLR Falcon research aircraft. The encountered ultrathin subvisual cloud layers can be characterized as (1) horizontally extending over several hundred kilometers, (2) persisting for at least 3 hours (but most likely much longer), and (3) having geometrical thicknesses of 100–400 m. These cloud layers belong to the geometrically and optically thinnest ever observed. In situ particle size distributions covering diameters between 0.4 and 23 μm obtained from these layers are juxtaposed with those obtained inside cloud veils around cumulonimbus (Cb) anvils and also with background aerosol measurements in the vicinity of the clouds. A significant number of particles with size diameters around 10 μm were detected inside these ultrathin subvisible cloud layers. The cloud particle size distribution closely resembles a background aerosol onto which a modal peak between 2 and 17 μm is superimposed. Measurements of particles with sizes above 23 μm could not be obtained since no suitable instrument was available on Geophysica. During the flight of 6 March 1999, upper tropospheric and lower stratospheric background aerosol was measured in the latitude band between 4°S and 19°S latitude. The resulting particle number densities along the 56th meridian exhibit very little latitudinal variation. The concentrations for particles with sizes above 0.5 μm encountered under these background conditions varied between 0.1 and 0.3 particles/cm³ of air in altitudes between 17 and 21 km.

INDEX TERMS: 0305 Atmospheric Composition and Structure: Aerosols and particles (0345, 4801); 0320 Atmospheric Composition and Structure: Cloud physics and chemistry; 0365 Atmospheric Composition and Structure: Troposphere—composition and chemistry; 4801 Oceanography: Biological and Chemical: Aerosols (0305); **KEYWORDS:** subvisual, cirrus, tropics, tropopause, background, aerosol

Citation: Thomas, A., et al., In situ measurements of background aerosol and subvisible cirrus in the tropical tropopause region, *J. Geophys. Res.*, 107(D24), 4763, doi:10.1029/2001JD001385, 2002.

¹Institut für Physik der Atmosphäre, Universität Mainz, Mainz, Germany.

²Max-Planck-Institut für Chemie, Mainz, Germany.

³Institut für Physik der Atmosphäre, DLR, Oberpfaffenhofen, Germany.

⁴Istituto di Scienze dell'Atmosfera e del Clima, CNR, Rome, Italy.

⁵Institut für Meteorologie und Geophysik, Universität Frankfurt, Frankfurt, Germany.

⁶Institut für Chemie und Dynamik der Geosphäre (ICG-1), Forschungszentrum Jülich GmbH, Jülich, Germany.

⁷Myasishchev Design Bureau, Moscow, Russia.

⁸Istituto di Ricerca sulle Onde Elettromagnetiche, CNR, Florence, Italy.

⁹Observatoire Cantonal, Neuchâtel, Switzerland.

¹⁰Central Aerological Observatory, Moscow, Russia.

¹¹Environmental Science Department, Lancaster University, Lancaster, UK.

1. Introduction

[2] Subvisual cirrus clouds are known since the early 1970s mainly through lidar measurements [Uthe and Russell, 1977; Heymsfield, 1986]. These clouds, frequently occurring near the local tropopause, often are of considerable horizontal extent. For this reason they possibly play a role in dehydration and the mechanisms behind the dryness in the lower stratosphere. Also the cloud particles could influence the gas phase chemistry by heterogeneous reactions. Knowledge of the particle sizes and other microphysical properties, chemical composition and formation mechanisms of these clouds is very limited, because only few results of in situ measurements are available in the literature.

1.1. Definitions and Phenomenology

[3] Cloud layers of a few hundred meters to 1 km thickness occurring in the vicinity of the tropical mean tropopause, horizontally extending over up to 2700 km were reported by Winker and Trepte [1998] based on LITE (Lidar In-space Technology Experiment) measurements. Observations showed them as thin sheets of unusual homogeneity in clear air, frequently above intense tropical thunderstorms. By comparing midlatitude lidar measurements of subvisual clouds with visual cirrus, Sassen *et al.* [1989] defined clouds as subvisual, if their optical thickness τ_c is below $\tau_c \approx 0.03$ at visible wavelengths. Schmidt *et al.* [1993] and Schmidt and Lynch [1995] used as threshold criterion a visible optical depth of $\tau_c \leq 0.05$ and introduced, mainly based on possible cloud formation mechanisms, five classes of subvisual clouds. These are (1) equatorial/Intertropical Convergence Zone (ITCZ) clouds, (2) clouds of origin near jet streams, (3) clouds associated with cold fronts, (4) orographically generated subvisual clouds, and (5) other types like anvil top clouds or contrail residues. They estimated cloud persistence times ranging from minutes for “class 5” to days for “class 1.” SAGE II extinction observations of zonally averaged occurrence frequencies of subvisual cirrus clouds are given by Wang *et al.* [1996] for latitudes ranging from -60°S to $+60^\circ\text{N}$. The measured 6-year climatology clearly demonstrates the existence of such clouds in this entire latitude band, both above and below the average tropopause location, with an occurrence frequency maximum in the tropics.

1.2. Microphysical Properties

[4] Adopting $\tau_c \leq 0.05$ as threshold for the visible optical depth, Lynch [1993] proposed the following as “baseline properties”: Subvisual cirrus clouds consist of nonspherical ice particles like plates, columns, bullets, or clusters having long dimension sizes smaller than $50\text{ }\mu\text{m}$, and are of number densities below 50 L^{-1} with an ice water content (IWC) not above $2 \times 10^{-1}\text{ mg/m}^3$ (These number were obtained by ASSP measurements with a lower size detection limit of $3\text{ }\mu\text{m}$). The clouds occur at altitudes between 12 and 18 km at or near the tropopause and have geometrical thicknesses below 1 km. Similarly Schmidt *et al.* [1993] quote liquid or ice water contents of $0.08\text{--}0.2\text{ mg/m}^3$ for subvisual ITCZ cirrus clouds with the exception of their “class 4,” where significantly higher values ($0.2\text{--}1.0\text{ mg/m}^3$) can be reached. Sassen *et al.* [1989] also derived estimations of cloud particle sizes (based on a low number of observations at midlatitudes and assuming small hexagonal ice crystals) to be on average near $25\text{ }\mu\text{m}$ effective diameter. For number

concentrations they provide values near 25 L^{-1} . Barnes [1980] presented in situ observations of large particles in clear air at midlatitude and tropical latitudes when flying under cirrus clouds and labeled these as subvisible cirrus. The largest sizes obtained with a PMS 1D probe were around $200\text{ }\mu\text{m}$ and concerning the number density it is stated “Generally, the maximum concentrations in cloudless skies have been 10^4 counts/m^3 with the peak in the distribution in the $2\text{--}10\text{ }\mu\text{m}$ range as determined by the ASSP.” In situ measurements by Heymsfield [1986] in thin layers of cirrus clouds above the (tropical) Marshall islands between 16.2 and 16.7 km altitude utilizing a formvar replicator showed a 50% mixture of trigonal plates and columns at inside cloud temperatures of -83°C to -84°C . The trigonal plates detected had thickness to diameter ratios of nearly 1.0 at small sizes. The sizes detected by the replicator range from the lower detection limit of $5\text{--}50\text{ }\mu\text{m}$. Concurrent ASSP measurements showed mean concentrations throughout the layer of 0.05 cm^{-3} (i.e., 50 L^{-1}) and the mean diameter was estimated to $5\text{ }\mu\text{m}$ with IWC typically around 10^{-1} mg/m^3 . Knollenberg *et al.* [1993] adopted a combination of modified Forward Scattering Spectrometer Probe (FSSP)-100 and 2D probe to measure ice crystals in cumulonimbus (Cb) anvils over Micronesia and concluded for the smaller crystals that these “are quite dense and quasi spherical or of low aspect ratio.” The size distributions exhibit a peak at $20\text{ }\mu\text{m}$ with number densities expressed as dN/dD below $10^{-2}\text{ cm}^{-3}\text{ }\mu\text{m}^{-1}$ at temperatures near -40°C . In situ measurements from the Marshall Islands (December 1973) presented by McFarquhar *et al.* [2000] showed that no crystals larger than $17\text{ }\mu\text{m}$ were detected by the ASSP (size detection range: $2\text{--}30\text{ }\mu\text{m}$), while the presence of particles as large as $20\text{--}50\text{ }\mu\text{m}$ was indicated by a 1DC probe. Other investigations by McFarquhar and Heymsfield [1996] show that large ice particles in tropical anvil clouds are of quasi-circular and hexagonal platelike shape. Their Video Ice Particle Sampler (VIPS) analyses furthermore show that over 90% of those crystals with sizes from $5\text{--}10$ to $100\text{ }\mu\text{m}$ are quasi-circular in shape exhibiting rounded edges. They also concluded that the observed particle habits inside tropical cirrus significantly differ from those commonly found in midlatitude cirrus clouds.

1.3. Suggested Mechanisms for Cloud Formation

[5] Although a variety of possible mechanisms for creating and supporting such clouds have been introduced in the literature, this question still seems unresolved requiring more measurements and theoretical discussion.

[6] Barnes [1980] diffusely conjectured “natural lifting motions within the atmosphere” as cloud generation mechanism. By means of satellite measurements over convectively active areas like the ITCZ region, Prabhakara *et al.* [1988] observed that thin cirrus clouds were present $100\text{--}200\text{ km}$ away from high-reaching thick clouds. They suggested that the cold tops of such thick clouds possibly are the source of spreading thin cirrus sheets. In opposition to this view, Heymsfield [1986] observed thin cirrus at the tropopause in absence of convection. Jensen *et al.* [1996a] assume for the formation of thin cirrus that either these layers are residues of cirrus outflow from deep convection cloud anvils, or that such layers form at the tropical tropopause by the slow synoptic scale uplifting of a moist air layer and



Figure 1. The Russian high-altitude research aircraft “Geophysica” before takeoff on the airport of Mahé, Seychelles. The mounting of the FSSP-300 sonde underneath the left wing is shown in the small photo.

homogeneous nucleation. For the outflow scenario ice particle equivalent volume radii between 2 and 20 μm result for the matured clouds. For the slow-uplifting-scenario peak ice crystal number densities of 0.5 cm^{-3} and equivalent volume radii of 4–10 μm result with visible optical depth of 0.02. Also *Jensen et al.* [1996b] performed simulations of the tropical ice cloud formation in the temperature minima of gravity waves using wave periods of 1–2 hours. The results indicate that high numbers of ice crystals with sizes between 2 and 4 μm radius can form due to the low temperatures and rapid cooling. With respect to the availability of sufficient water vapor, *Jensen et al.* [1999] presented water vapor measurements with error analysis from the Microwave Limb Sounder on the UARS (Upper Atmospheric Research Satellite). These show relative humidities often reaching near saturation with respect to ice in the tropical upper troposphere. The detected humidity values cover large-scale areas and an uplift with cooling by a few hundred meters suffices for ice nucleation and growth, as well as for supporting formation and persistence of thin cirrus.

1.4. Modeling of the Cloud Properties

[7] Some of the observational results have found entry into model calculations. For example, *Boehm et al.* [1999] implement initial ice particle size distributions for modeling the nighttime conditions of cirrus outflow remnants in the tropics with modal radii of 10 and 20 μm based on the measurements by *Knollenberg et al.* [1993] and *McFarquhar and Heymsfield* [1996]. These model calculations suggest, that ice crystals in tropical cirrus must have modal radii less than 10 μm , because otherwise the cloud lifetime would be too small in comparison with the observations. Using lognormal size distributions of varying modal parameters for subvisual tropical cirrus, *Rosenfield et al.* [1998] conclude that 2 μm particles lead to scattering ratios above those observed by lidar. If size radii of 6 μm are tried instead, the observations match the calculated backscatter ratios and optical depths.

[8] It has to be noted that tropical subvisual clouds occur at the tropopause in an environment characterized by temperatures below -80°C , while at midlatitudes these temperatures are not much less than -60°C . Therefore

cloud particle habits and microphysical properties in tropical clouds might differ from those at midlatitudes.

1.5. Chemical Composition and Effects

[9] Concerning the chemical composition of the subvisual cloud particles, *Hamill and Fiocco* [1988] suggested that tropical atmospheric conditions allow for NAT (Nitric Acid Trihydrate) particles to remain stable. *Omar and Gardner* [2001] tried to supply experimental evidence for this by means of spaceborne lidar measurements. Most of the references quoted implicitly or explicitly assume that the particles detected in the subvisual cirrus clouds consist of ice as main constituent.

[10] Since the subvisual clouds frequently occur at or even above the tropopause [*Wang et al.*, 1996; *Winker and Trepte*, 1998] heterogeneous chemical reactions on the cloud particles could play a role for the chemical composition of the air in this region. Such chemistry could for example affect the ozone or NO_y abundances [*Borrmann et al.*, 1996; *Solomon et al.*, 1997] in the tropopause region. For chlorine related reactions to proceed efficiently already low values of reactive particulate surface area suffice, as has been shown by *Fahey et al.* [1993], and *Keim et al.* [1996] provided the involved reactive uptake coefficients are high as is the case for particles consistent of ice. Therefore thin populations of small particles like represented by subvisual cirrus clouds could play a role in this respect. For this issue, which is a matter of current debate [e.g., *Bregman et al.*, 2002], also detailed knowledge of the chemical composition of the cloud particles is critical.

1.6. Tropical In Situ Measurements During the 1999 Airborne Polar Experiment-Third European Stratospheric Experiment on Ozone (APE-THESEO) Campaign

[11] The APE-THESEO campaign (described by L. Stefanutti et al., The APE-THESEO tropical campaign, submitted manuscript, 2002) was carried out from 19 February to 11 March 1999, utilizing the Russian M-55 high-altitude

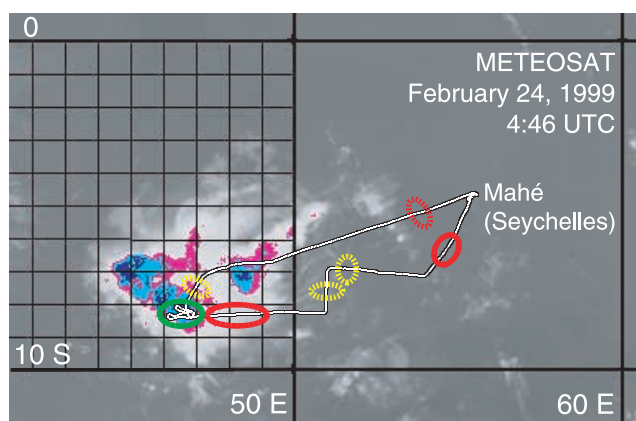


Figure 2. Meteosat IR image of the Cb cloud from 24 February 1999, where the visible outflow region approximately corresponds to the white area. The Geophysica flight path is traced in black, and the various colored areas correspond to cloud penetrations where in situ data were obtained (see text for details). Decreasing cloud top temperatures are color coded from purple toward dark blue.

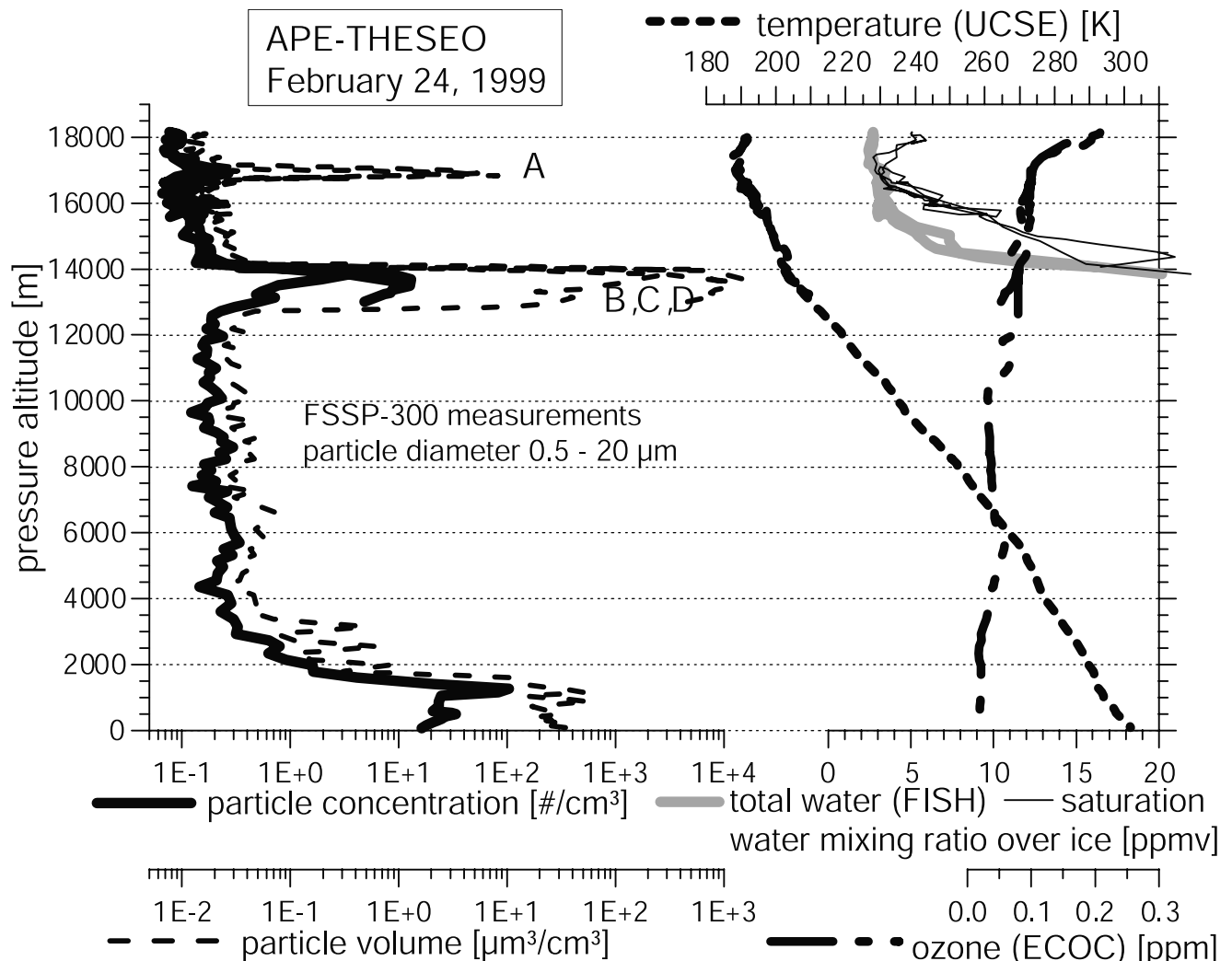


Figure 3. Vertical profiles of temperature, ozone and water vapor mixing ratios, and measured aerosol properties for the flight of 24 February 1999. The thin black line indicates the water vapor mixing ratio necessary for saturation with respect over ice at the encountered ambient conditions. The thick light gray line depicts the total water vapor measurements from FISH. In the cloud regions, these two lines coincide, thus indicating saturation.

research aircraft Geophysica [Stefanutti *et al.*, 1999] and the DLR Falcon, both based on the island of Mahé (Seychelles, 55°31'E longitude, 4°40'S latitude). The purpose of this paper is to present in situ particle size distribution measurements obtained during this campaign from ultrathin tropical tropopause subvisual cirrus clouds, the outermost regions of various anvil outflow clouds, cloud patches near a Cb turret, as well as background aerosol measurements in the tropical upper troposphere and lower stratosphere. For this study the data of coordinated concurrent Geophysica and DLR Falcon flights from 24 to 27 February 1999 are used. Additionally size resolved aerosol measurements of the tropical upper tropospheric and lowermost stratospheric background atmosphere are presented utilizing the data of the 6 March 1999 Geophysica flight.

2. Methodology

[12] The aerosol particle size distributions were measured in situ on board of Geophysica by means of a FSSP-300

optical particle detection instrument covering a particle diameter size range from roughly 0.41 to 23 μm (dependent on the refractive index of the particles) in 31 size bins [Baumgardner *et al.*, 1992]. Specific arrangements were implemented to ensure the instrument's operation extending over the moist, hot ground conditions to the dry, cold conditions ($\approx -90^\circ\text{C}$) encountered in the tropical tropopause region and to enable transitions between these extremes within 25 min. The FSSP-300 pod installation under the left wing of Geophysica is shown in Figure 1. The data acquisition and control computer was mounted in a specially designed unpressurized, thermally controlled container box inside the airplane's wheel compartment.

[13] The conversion of the individual particle light scattering signals to particle sizes was performed adopting Mie theory for background aerosol conditions, while for the cloud encounters the T-matrix method was applied according to the study of Borrmann *et al.* [2000]. An optical refractive index of 1.44 was assumed for the stratospheric

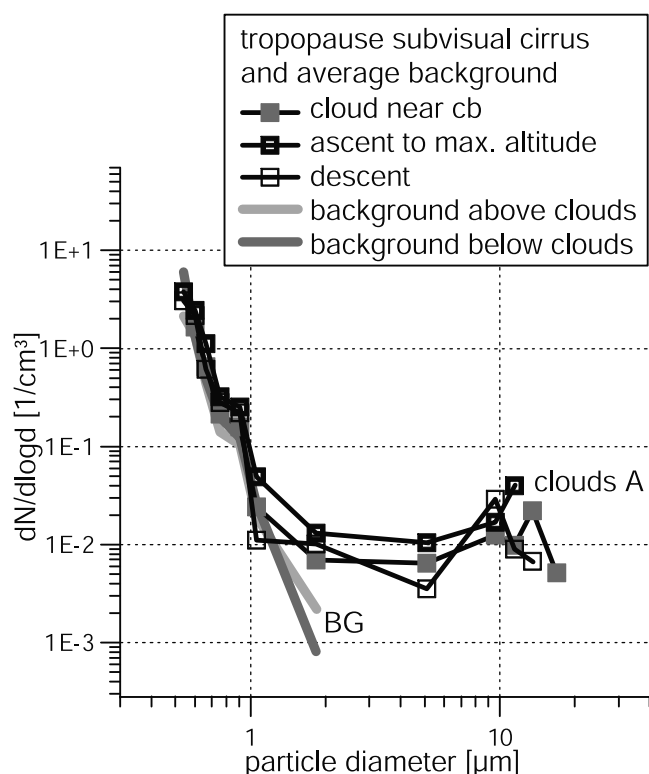


Figure 4. Size distributions of the subvisual cloud layer (labeled as “A” in Figure 3) at the tropical tropopause near 17 km. Due to counting statistics, the three curve segments do not significantly differ from each other at sizes above 2 μm . The curves labeled “BG” correspond to background aerosol measurements outside of (but close to) the cloud.

and uppermost tropospheric sulfuric acid aerosol background particles. This implies a certain simplification because Geophysica did not fly high above the tropical tropopause region and therefore particles other than sulfuric acid droplets might have been sampled also. However, the particle size channels as given by the instrument above 0.9 μm are wide because due to the “Mie-ambiguities” several size bins have to be combined here to wider channels. Thus a some variation of the refractive index (either due to dilute versus concentrated sulfuric acid droplets or particles of different composition) will not result in greatly changed size distributions. For the aspherical cirrus cloud particles the T-matrix calculations were performed using 1.31 as refractive index for ice. Despite hypotheses concerning the chemical composition of the cloud particles suggesting that nitric acid may be involved, for this study the sampled particles are assumed to be ice. This mainly because the concurrent in situ total water measurements on Geophysica indicate saturation or supersaturation with respect to ice for all cloud events analyzed. For the particle shape rotationally symmetric ellipsoids with an axis length ratio of 0.8 were assumed.

[14] The data frames taken for each sample were of 2–5 s accumulation time. Before deriving particle size distributions all entering data frames recorded inside clouds with this high resolution were individually inspected for possible artifacts introduced by the presence of larger cloud particles

(i.e., with sizes beyond the upper detection limit of the FSSP-300). None of the sampling data frames taken from the clouds of 24 and 27 February 1999 were affected by this kind of error. Also based on the presence of particles larger than 5 μm , it was decided during these frame-by-frame inspections whether a data reduction using Mie theory or the T-matrix method was adopted in order to differentiate between inside-cloud and background aerosol data sets. Commonly out of the 2–5 s data frames larger flight time intervals of at least 60 s had to be averaged together for the FSSP-300 data due to the very low atmospheric particle number densities and the corresponding demands of counting statistics.

[15] It is important to note that the upper size detection threshold of the FSSP-300 arrangement is near 23 μm , which implies certain limitations. In cirrus decks connected with anvils larger particles may be present albeit in much

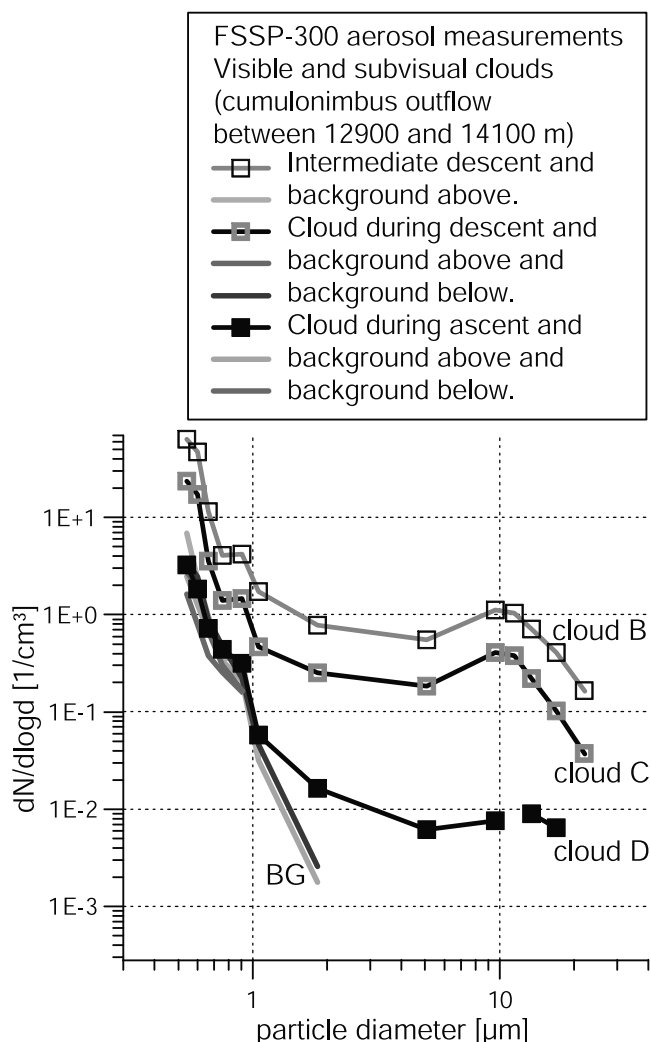


Figure 5. Size distributions of three different parts of a Cb outflow cirrus. “Cloud B” and “Cloud C” qualify as visible based on their optical depths. Based on the FSSP-300 data, “Cloud D” would be subvisual. However, if larger particles were present, the optical thickness might be higher. The letters “B,” “C,” and “D” correspond to the data with the same label in Figure 3.

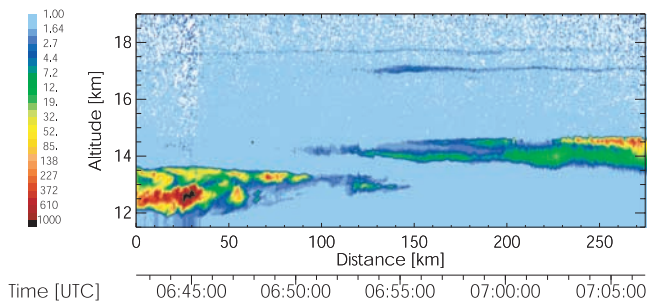


Figure 6. OLEX lidar observations in terms of geometrical altitude during the last flight leg (descent) of the 24 February 1999 flight. The backscatter ratio at 1064 nm is color coded and displayed as vertical cross section through the atmosphere above the aircraft. The backscatter ratio is defined for this figure as the ratio of total (aerosol plus air molecular) backscatter coefficient divided by pure air molecular backscatter coefficient.

lower number densities [Heymsfield and McFarquhar, 1996]. For this reason the size distribution measurements presented in this study for Cb outflow clouds highlight the properties of the smallest hydrometeors only. Also the optical properties derived from the size distribution measurements pertain to the size limits inherent in the FSSP-300 design. However, with regard to possible heterogeneous chemistry effects the particulate surface area supplied by the small sized particles may be sufficient to drive certain reactions near saturation [Fahey *et al.*, 1993; Keim *et al.*, 1996].

[16] Besides these in situ aerosol measurements, the remote sensing instruments MAL (Miniature Airborne Lidar) and MAS (Multiwavelength Aerosol laser Scatterometer) probed the near range around the aircraft. MAL is a microjoule lidar operating at 532 nm [Matthey *et al.*, 2000] and capable of parallel and perpendicular polarization of the backscattered light signal. MAS is an instrument similar to a backscatter sonde using three different wavelengths [Adriani *et al.*, 1999] and delivers time series of backscatter ratio (BSR) as well as depolarization ratio (DR). Measurements performed by means of the FISH (Fast In situ Stratospheric Hygrometer) instrument [Zöger *et al.*, 1999] delivered total water data, i.e., the sum of gas phase and particulate water. The ozone mixing ratio was measured by an electrochemical cell sensor (ECOC) from the Central Aerological Observatory (CAO) in Moscow [Kyrö *et al.*, 2000] and N_2O was measured as tracer gas by HAGAR [Riediger *et al.*, 2000]. The altitudes given in this study for the in situ measurements are pressure altitudes.

[17] For the flights of 24 and 27 February 1999, as well as on 6 March 1999, the meteorological research aircraft Falcon of DLR (German Aerospace Center) preceded Geophysica performing lidar measurements above 10 km. On board of the Falcon the 4-wavelength aerosol and ozone lidar, Ozone Lidar Experiment (OLEX) was installed zenith-viewing [Wirth and Renger, 1996]. It provided 2D vertical cross sections of cirrus and subvisible cirrus cloud backscatter ratio at 354, 532 and 1064 nm, of the depolarization at 532 nm and of stratospheric ozone along the flight path. By means of these measurements Geophysica, usually taking off 30 to 60 min after the DLR Falcon, could

be guided by the Falcon crew into regions with clouds of interest.

3. Subvisual Clouds Near the Tropical Tropopause

[18] On 24 February 1999 a Cb cloud system of approximately 400 km diameter was studied by means of concurrent, coordinated Falcon (remote sensing measurements) and Geophysica (in situ instrumentation) flights. In situ aerosol measurements were obtained: (1) at the margin of the main cloud body between 14.1 and 15.3 km altitude, (2) in the outermost regions of the outflow cirrus umbrella between 12.9 and 14.1 km, (3) the subvisual cloud layer at 16.9 km above (albeit disconnected from) the Cb system. The size

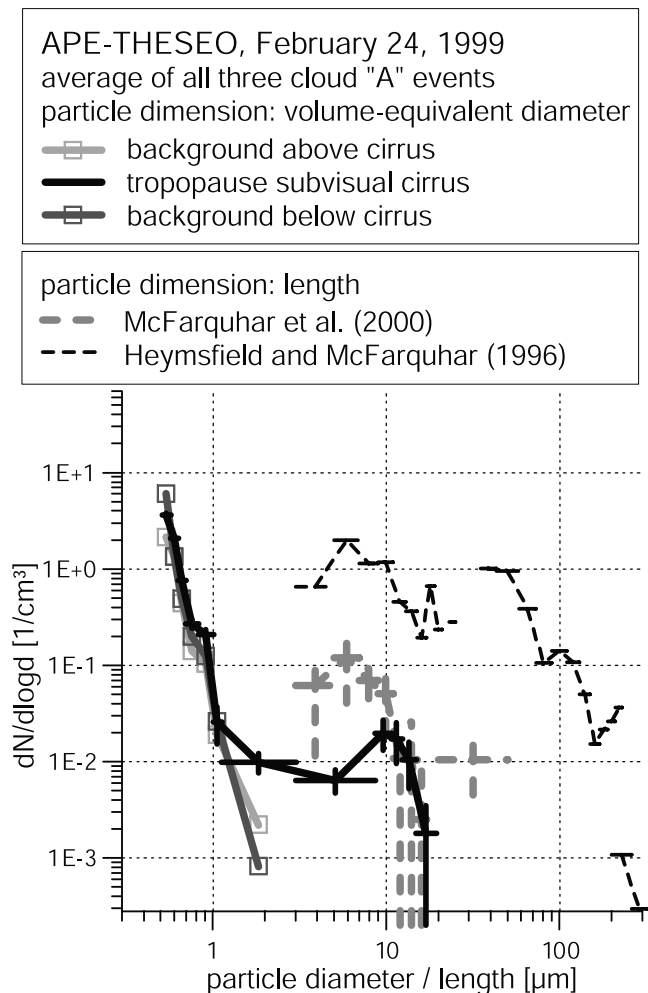


Figure 7. Composite of FSSP-300 size distribution measurements inside the tropical subvisual tropopause cirrus layer “A” (see Figures 3 and 4) on 24 February 1999. The in situ data of McFarquhar *et al.* [2000] and Heymsfield and McFarquhar [1996] from the Marshall Islands are entered for comparison. The horizontal bars in these curves represent the width of the instrument’s size bins. The vertical bars in the black, solid curve designate the errors due to counting statistics. The vertical dashed gray bars in the upper McFarquhar *et al.* [2000] data indicate the variability over several measured sampling periods.

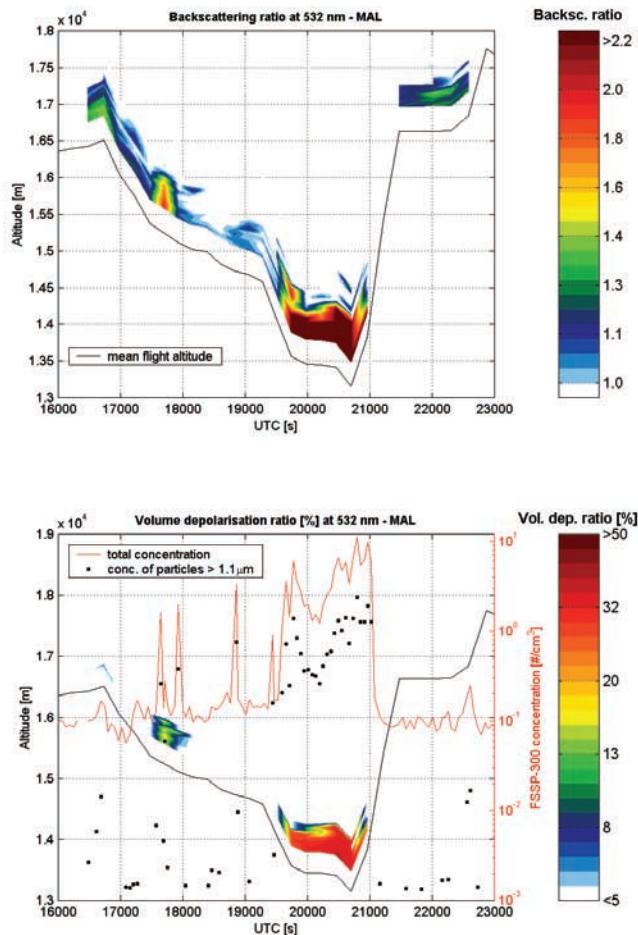


Figure 8. Synopsis of MAL and FSSP data for events “Cloud A” and “Cloud B” of the 24 February 1999 flight. (See text for detailed discussion.)

and location of this Cb system, as well as the flight path of Geophysica and the relative positions of the cloud samples can be inferred from the Meteosat image of Figure 2. The areas colored in green correspond to (1), in red/brown to (2), and in yellow to (3).

[19] The vertical profiles from the second half of the Geophysica flight of 24 February 1999 (including the descent) for aerosol number density and particulate volume are shown in Figure 3 as measured by the FSSP-300. Additionally ozone, the ambient temperature, and total water content are displayed, this way identifying the location of the local tropopause near 17–17.5 km pressure altitude. Two distinct cloud layers are discernible: one geometrically thick layer between 12.2 and 14.2 km altitude (labeled as “B,” “C,” and “D”), and a second one located at 16.8 km (labeled as “A”). The cloud particle size distributions shown in Figure 4 correspond to this upper layer “A,” while the size distributions “B,” “C,” and “D” of Figure 5 are from the layer between 12.2 and 14.2 km. The upper cloud layer “A” had a vertical extent of 100–400 m (being 100–200 m most of the sampled time) and constitutes a subvisible cirrus cloud since its optical depths based on Mie theory calculations are between 0.0004 and 0.0005 for 632 nm wavelength and between 0.0002 and 0.0003 for 11 μm. These optical thicknesses fall below the

thresholds of 0.05 in the visible and 0.03 in the infrared for distinction of visual from subvisual cirrus clouds as suggested by *Schmidt et al.* [1993]. The derived optical thickness also satisfies the threshold criteria proposed by *Sassen et al.* [1989]. Since there is the possibility of the presence of particles larger than the FSSP-300s upper detection limit (of about 23 μm), the optical thicknesses derived for the 24 February 1999, cloud constitute lower limits. However, considering the fact that this cloud was less than 400 m thick and persisted for at least 3 hours, particles much larger than 23 μm would have sedimented out. Particles larger than 20 μm diameter have under the measured atmospheric conditions sedimentation velocities in the range of a few hundred meters per hour [e.g., *Knollenberg et al.*, 1982]. Therefore it is unlikely that large numbers of particles above the upper detection limit of the FSSP-300 are present in the cloud events of 24 February 1999.

[20] While the size distributions of Figure 4 are tropopause subvisual cirrus clouds, those in Figure 5 are from three different parts of a Cb outflow umbrella region. The 1064 nm data from the DLR OLEX lidar in Figure 6 actually show two disjunct layers between 16 and 18 km above the anvil outflow clouds between 12 and 15 km. The lower, thicker cloud near 12–15 km geometric altitude roughly corresponds to the lower layer (labeled as “B,” “C,” and “D”) in Figure 3 and constitutes the cirrus umbrella in the outflow of this mesoscale Cb system. As described by *Santacesaria et al.* [2002] for a similar case of the APE-THESEO flight from 19 February 1999, the upper layer on 24 February 1999, near 16 km was

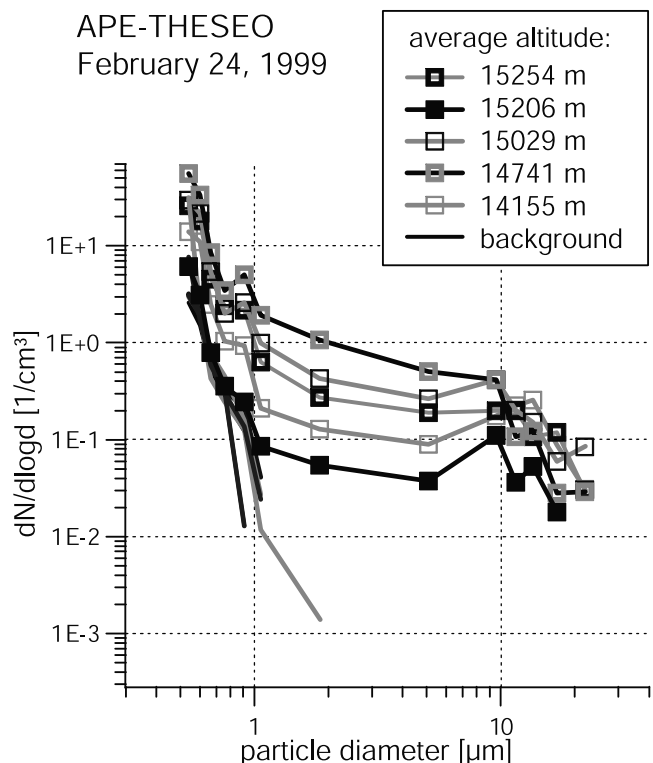


Figure 9. Measurements of cloud particle size distributions in cloud patches near the margins of the Cb main cloud as well as from the surrounding clear air background aerosol (24 February 1999 flight).

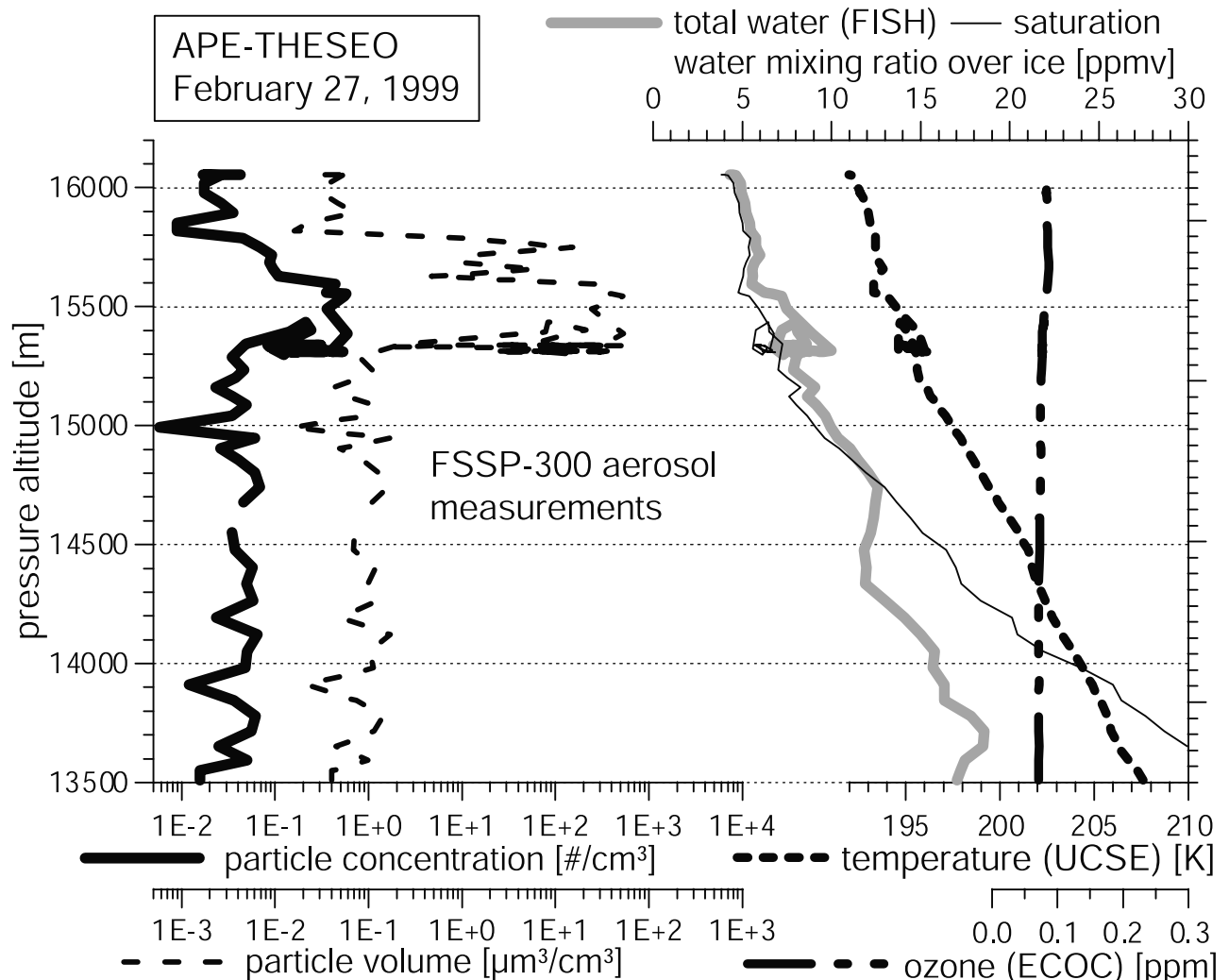


Figure 10. Profiles of measured temperature, ozone and water vapor mixing ratios, and aerosol properties for the flight of 27 February 1999. The thermal tropopause was at 16.8 km and the ozone started increasing from 70 ppbv toward stratospheric values at 17.0 km. Saturation with respect to ice is indicated within (and below) the cloud regions as in Figure 3.

significantly above the Cb cloud and entirely disconnected. The picture of the DLR OLEX lidar in Figure 6 shows that these ultrathin cirrus layers horizontally extend over more than 250 km. These two layers do not appear on the corresponding, concurrent lidar data at 532 and 354 nm. Only one of them (see the size distribution labeled as “A” in Figure 4) was penetrated by Geophysica. It needs to be noted that the Falcon and Geophysica could not sample entirely identical air masses because Geophysica did not fly exactly along the path traced out by the Falcon’s lidar beam. Either the planes were horizontally separated by approximately 20 km or they reached the cloud at nearly the same position albeit separated in time by 45 min. The subvisual cirrus layer directly underneath the tropical tropopause was penetrated three times by Geophysica within 2 hours.

[21] The size distributions of the three individual penetrations in Figure 4 are not significantly different from each other and all three were obtained at different pressure altitudes but at identical potential temperature (i.e., 377 K). However, since the counting statistics of each event is poor,

a single, composite, size distribution has been made for Figure 7 from the data of these three crossings. Otherwise the size resolution of the FSSP-300 data would have to be decreased, which would result in size bins wider than those commonly used by *Baumgardner et al.* [1992] or *Borrmann*

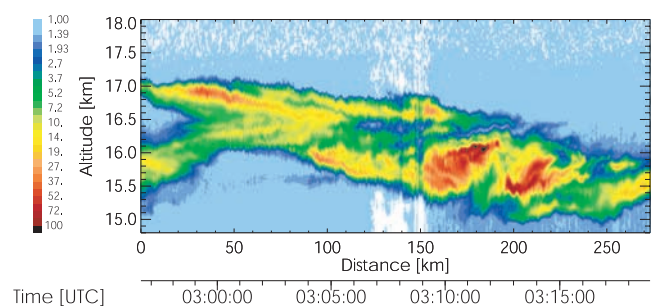


Figure 11. OLEX lidar observations in terms of geometrical altitude during the flight of 27 February 1999, near the region where Geophysica obtained in situ data.

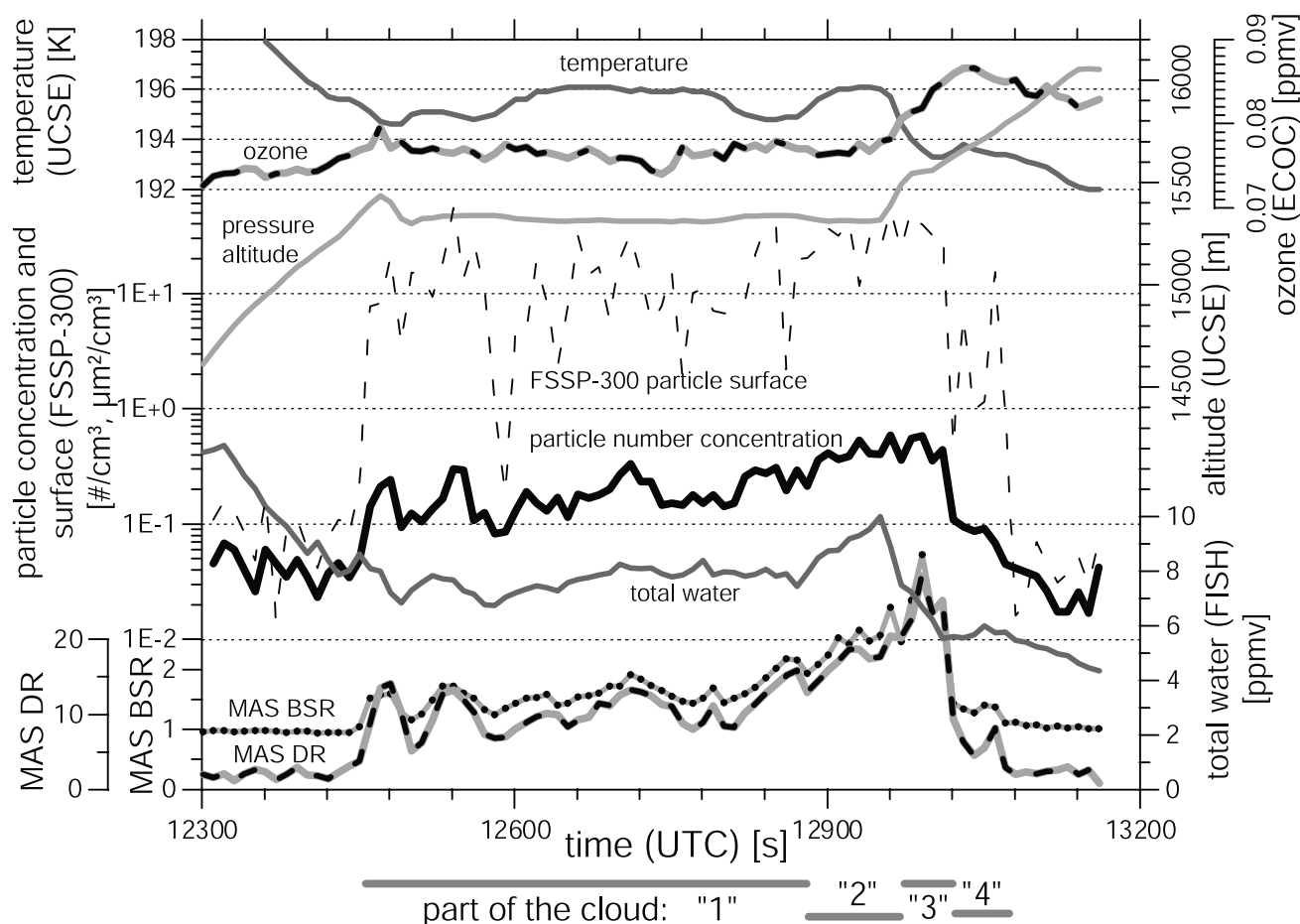


Figure 12. Time series of MAS (BSR: backscattering ratio, DR: depolarization ratio at 532 nm), FSSP-300, FISH, and ECOC data for the cloud event of 27 February 1999.

et al. [2000]. The size distribution significantly differs from the background aerosol of the surrounding air as shown in Figure 4 (and labeled there as “BG”), but only for size diameters larger than $1\ \mu\text{m}$. Although the number densities are as low as $0.011\ \text{particles}/\text{cm}^3$ (i.e., $11\ \text{L}^{-1}$) for sizes above $1\ \mu\text{m}$, a distinct peak around $10\ \mu\text{m}$ is present inside this cloud. If all particles detected by the FSSP-300 down to $0.57\ \mu\text{m}$ are taken into account, cloud particle number densities of $0.17\ \text{particles}/\text{cm}^3$ (i.e., $170\ \text{L}^{-1}$) of air result. Also entered into Figure 7 are data of December 1973 by Heymsfield and Jahnsen [1974, see McFarquhar *et al.*, 2000] and Heymsfield and McFarquhar [1996] from subvisual tropopause cirrus for comparison. These subvisual clouds over the Marshall Islands apparently also contained particles as large as $10\ \mu\text{m}$ although the peak of the size distribution is shifted toward smaller sizes compared with the 24 February 1999, case over the Indian Ocean. The measurements of the upper curve in this figure show much higher number densities over the entire size distribution and the presence of particles larger than $20\ \mu\text{m}$ as well. This cloud was qualified as subvisual by Heymsfield and McFarquhar [1996].

[22] The anvil outflow of the Cb cloud (see Figure 5) was also penetrated three times at different locations and at different stages in the cloud development. The shape of the size distributions with labels “Cloud B,” “Cloud C,”

and “Cloud D” is very similar for these three penetrations, only the absolute number concentrations change in dependency of the thickness of the cirrus veil around the Cb turret. The thickness of “Cloud B” was approximately $1100\ \text{m}$ with an optical depth at $632\ \text{nm}$ of 0.12 and of 0.082 at $11\ \mu\text{m}$. “Cloud C” was of similar geometrical thickness as “Cloud B,” but its optical depths were 0.037 for $632\ \text{nm}$ and 0.025 at $11\ \mu\text{m}$. The lowest curve in Figure 5 for “Cloud D” corresponds to a cloud layer of $650\ \text{m}$ vertical extent with 0.0008 ($632\ \text{nm}$) and 0.0005 ($11\ \mu\text{m}$) optical depths respectively. Thus for the upper two “Clouds B” and “C” the cloud thickness and optical depths were high enough to qualify as visual cirrus. The lowermost size distributions in Figure 5 labeled “BG” with particles smaller than $2\ \mu\text{m}$ only are background aerosol measurements taken immediately above and below this outflow cloud. The similarity of the three size distributions from the outflow cloud (designated as Cloud “B,” “C,” and “D”) may suggest a cause–effect relationship, however the database is insufficient to verify such a connection since the measurements were not quasi-Lagrangian.

[23] Figure 8 shows the time series of volume depolarization and backscattering ratio as measured by MAL for those parts of the flight of 24 February 1999, where “Cloud B” was within range of this instrument. The volume depolarization itself only can serve as a measure for the particle number

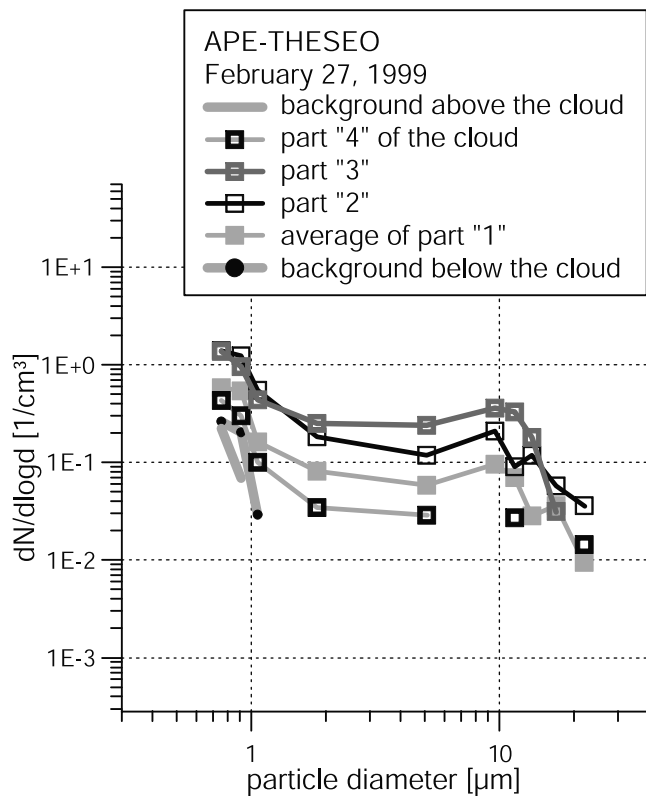


Figure 13. Cloud particle size distributions of the parts “1” to “4” in Figure 12 (see text for details).

density [Cairo *et al.*, 1999]. The short periods of enhanced number densities shown in the FSSP-300 data coincide with corresponding small increases of volume depolarization and scattering ratio in the figure. The aerosol depolarization also derived from these MAL measurements mostly were between 25% and 35%. This variable is a measure for the asphericity of the particles and based on the obtained values in this cloud it needs to be assumed that the FSSP-300 was confronted with particles of some asphericity. This justifies the application of the T-matrix method as mentioned above for the conversion of the scattered light intensities to particle sizes. It corresponds to results of McFarquhar and Heymsfield [1996] and Ström *et al.* [1997] who found slightly aspherical crystal habits for the smaller sizes.

[24] There are seven prominent features of the subvisual clouds encountered on 24 February 1999:

1. They are horizontally extending over several hundred kilometers.

2. The cloud lifetimes are at least 3 hours. This is the time interval when the planes were actually present in or under the cloud, and it can be speculated that the cloud persisted for a much longer period of time.

3. These cloud layers have geometrical thicknesses of 100–400 m, mostly even below 200 m. The optical depths are near 0.0004 at 632 nm.

4. The clouds occurred at ambient temperatures below 190 K.

5. These subvisual clouds exhibit a mode in the size distribution around 10 μm particle diameter.

6. and particles smaller than 1 μm have number densities of values near the background above and below the cloud.

7. The observed subvisual clouds more strikingly appear in the data of particulate surface area and volume than in the number densities.

The fifth item is consistent with the assumption by Boehm *et al.* [1999] who concluded based on radiative transfer model calculations and dynamical considerations, that the particles of such persistent tropical cirrus clouds should be smaller than 20 μm diameter and it is also consistent with other experimental findings mentioned in the Introduction. For example measurements with the FSSP-300 by McFarquhar and Heymsfield [1996] inside tropical cirrus clouds at altitudes between 7 and 14 km over the tropical Pacific also show a small mode between 10 and 20 μm . Similarly Knollenberg *et al.* [1993] report a small maximum between 10 and 20 μm for a Cb anvil penetration over Arizona, USA, while their measurements over Darwin, Australia, only exhibit a shoulder in the size distribution and not such a distinctive modal peak. Also in situ measurements by Heymsfield and Jahnsen [1974] inside tropical subvisual cirrus showed the enhanced presence of particles in the 3–17 μm size range.

[25] Although the similarity of the size distributions from clouds “A” (Figure 4) and “D” (Figure 5) seems indicative of a cause–effect relationship here too, again one can not necessarily conclude, that they have the same origin. Based on the wind speed and direction data measured by Geophysica as well as analyses of the meteorological data fields it becomes clear that the encountered cloud events are not from the same air mass like for a quasi-Lagrangian experiment.

[26] During the APE-THESEO flight of Geophysica on 24 February 1999, size distribution measurements also were obtained at the outermost margins of the Cb turret between

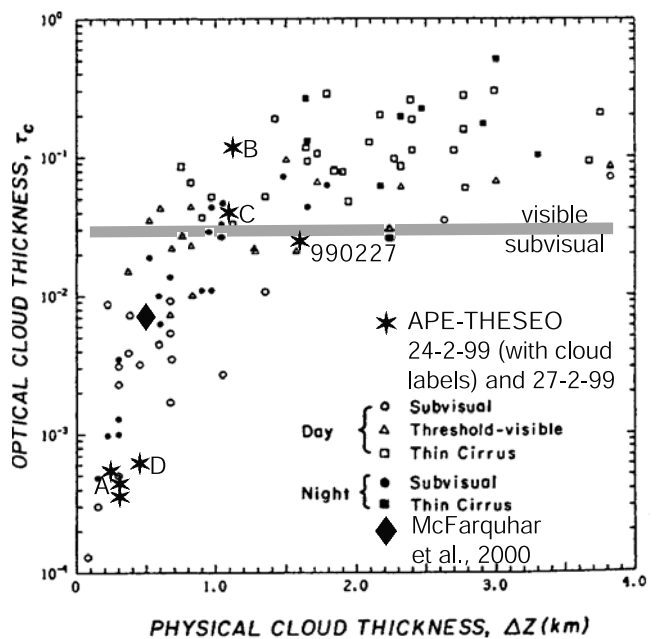


Figure 14. Optical thickness of visible and subvisual cirrus clouds from lidar measurements [Sassen and Cho, 1992]. In addition, the in situ data for the tropical regions of the Marshall Islands from 1973 [McFarquhar *et al.*, 2000] as well the Indian Ocean (Geophysica flights from APE-THESEO 1999) have been entered into this figure.

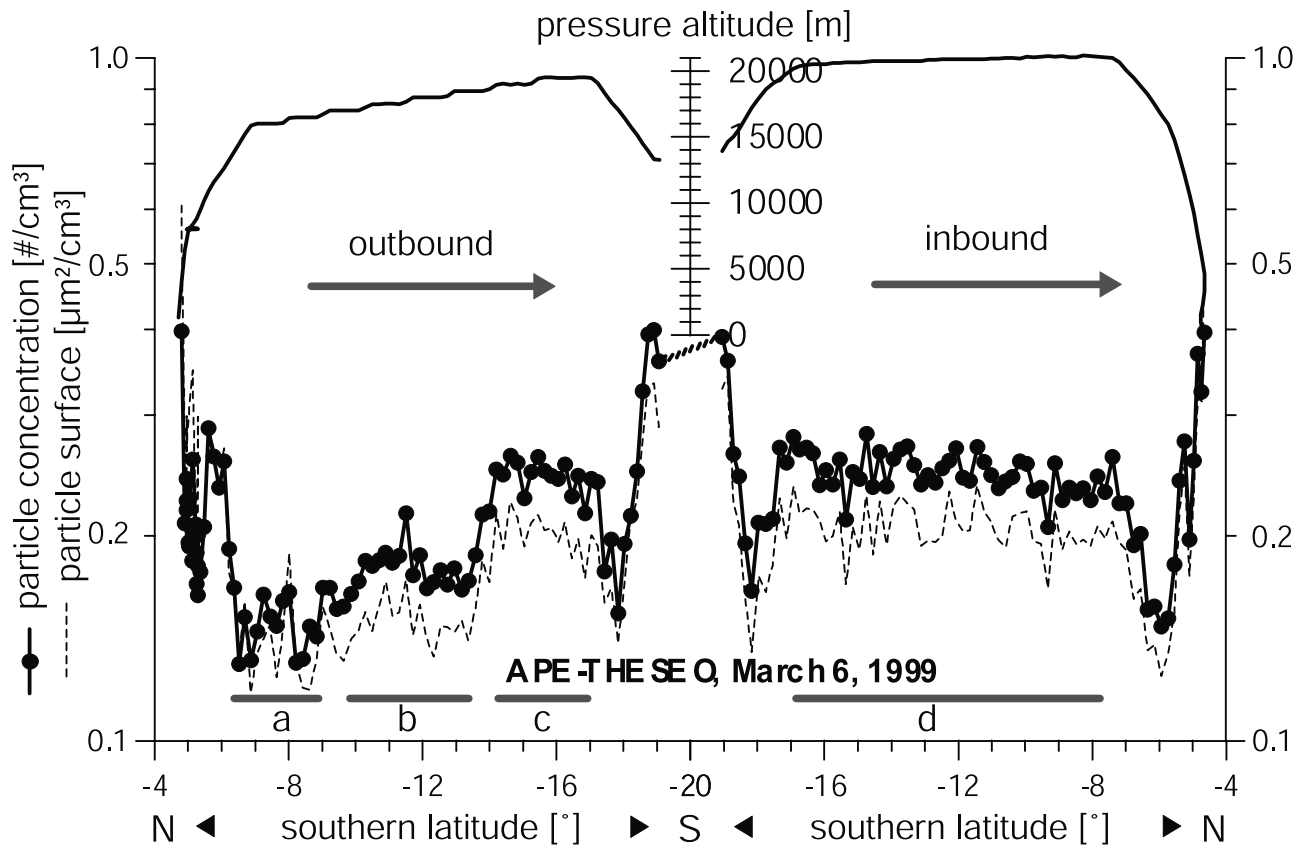


Figure 15. Flight cross section of the aerosol data along the 56th meridian from 6 March 1999. The flight segments labeled “a” to “d” are discussed in the text.

14.1 and 15.3 km altitude, the results of which are shown in Figure 9. In this part of the flight path Geophysica performed a slow descent. A large spatial inhomogeneity characterized by mostly clear air parcels with occasional interspersed patches of cloudy air was encountered in this area. Most likely this was a region of entrainment or detrainment. Since Geophysica could not penetrate deeper into the turret, only these cloudy patches could be sampled for periods of less than 60 s. Because of the inhomogeneity the particle concentrations vary over one order of magnitude in the size range between 0.5 and 10 μm . Although the shoulder at 10 μm particle diameter is a dominant feature in the measurements of Figure 9, it should be noted that the lack of an instrument detecting larger particles limits the capability of obtaining results concerning the entire cloud patch.

4. Below Tropopause Cirrus Clouds of 27 February 1999

[27] During the ascent from Mahé (Seychelles) of Geophysica on the flight of 27 February 1999, an extended, contiguous cirrus cloud was crossed between 15,200 and 15,700 m pressure altitude, where the cold-point tropopause was located at 16.8 km. The vertical profile of the aerosol related data, ozone, and temperature is shown in Figure 10. The corresponding OLEX lidar profile is shown in Figure 11 where the lidar measurements were obtained approximately 40 min before Geophysica reached this

cloud. A detailed view of MAS and FSSP-300 data is given together with in situ total water measurements and ozone in the time series of Figure 12. The data of the entire cloud event (starting at 12460 and ending 13070 s UTC) were subdivided into four parts (labeled as part “1,” “2,” “3,” and “4”) because the measured parameters of

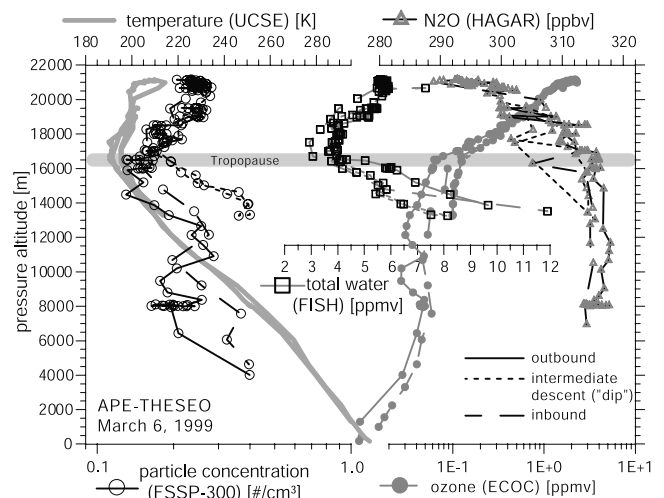


Figure 16. Vertical profiles of ozone, water vapor, N_2O mixing ratios, and aerosol concentrations from the entire flight of 6 March 1999. The tropopause region is indicated by the gray shadowed line.

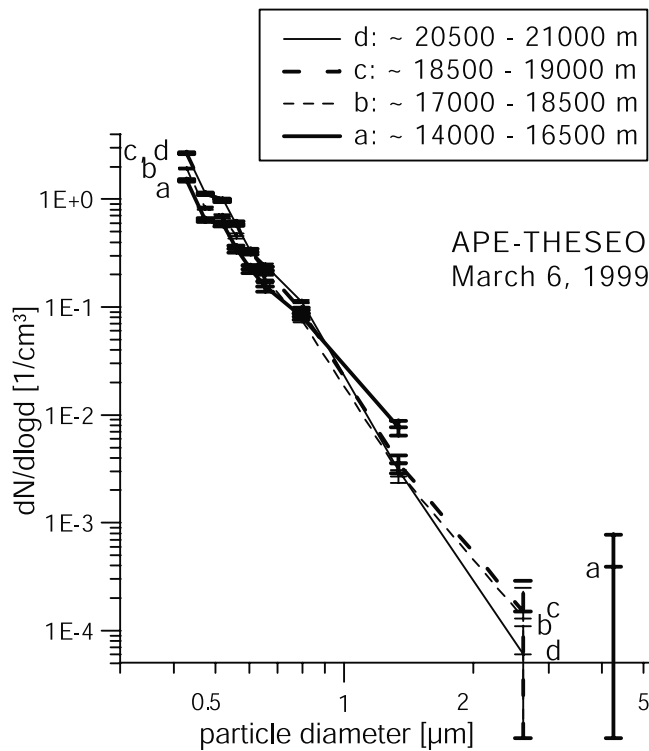


Figure 17. Particle size distributions of the background aerosol measured during the meridional cross section flight of 6 March 1999. The labeled curves correspond to the flight segments in Figure 15. The error bars designate the error due to counting statistics.

these parts significantly differ from each other. The four measured cloud particle size distributions are shown in Figure 13.

[28] In part “2” and especially in part “3” both of the MAS signals (also shown in Figure 12) are high compared to those obtained during part “4.” The lower particle number densities at sizes near $10\ \mu\text{m}$ in the particle size distribution of part “4” (see Figure 13) coincides with the decreased MAS signal, and the higher number density of part “3” is correlated with higher MAS BSR and DR. For parts “1” and “2” the ozone is lower while the total water

is higher than for parts “3” and “4.” The shapes of the size distributions (see Figure 13) are not very similar and these distributions differ most prominently in the absolute values of the particle number concentrations for sizes near $10\ \mu\text{m}$. Part “4” with the highest ozone levels and the lowest total water content exhibits greatly reduced number densities for these larger particles indicating increasing evaporation when approaching the tropopause.

[29] Utilizing the Lidar measurements for obtaining the geometrical thickness and using the in situ size distribution data, the optical thickness of the cloud parts can be roughly estimated. The highest value for the optical thickness resulting from such estimations for the entire cloud is 0.024 (0.015) for 632 nm ($11\ \mu\text{m}$). This is near the threshold differentiating between visible and subvisible cirrus. Considering also that larger particles most likely present in this cloud further enhanced the optical thickness, the cloud probably qualifies as visible cirrus.

[30] The optical cloud thickness of the various cloud encounters during the APE-THESEO campaign from the 24 and 27 February 1999 flights are shown in Figure 14 and placed into the context of previous [Sassen and Cho, 1992] lidar derived optical thicknesses for visible and subvisual cirrus. Also the data of McFarquhar *et al.* [2000] are entered into the figure. This comparison between in situ measurements and lidar data demonstrates that the subvisual clouds penetrated on 24 February 1999 are at the lowest level of previously measured optical and geometrical depths. The Geophysica measurements of the anvil outflow region from 24 February are near or just above the threshold value discriminating visual from subvisual and lie within the range of the other observations.

5. The Background Aerosol Between 5°S and 19°S Latitude in the Tropical Tropopause Region

[31] On 6 March 1999, a flight from Mahé at $5^{\circ}\text{--}19^{\circ}\text{S}$ was conducted due south along the 56°E longitude meridian. During this flight background conditions for aerosol were encountered in the upper troposphere and the lower stratosphere. The meridional cross section of the measured particle number density and surface area is shown in Figure 15. As can be seen from the pressure altitude data in this figure a “step ladder” profile across the tropopause

Table 1. Summary of the Observed Properties From the Encountered Clouds

Cloud type	Date	Pressure altitude [km]	Particle number density [number/cm ³] $0.7\ \mu\text{m} < d < 25\ \mu\text{m}$	IWC [mg/m ³] ^a	Geometrical thickness [m]	Optical depth $\tau_{632\ \text{nm}}$ ^a
Tropopause subvisual ci	24 February 1999	16.5–17.0	0.05	0.0033	300	0.0004
Cb outflow ci						
Subvisual	24 February 1999	13.2–13.9	0.04	0.0031	500	0.0007
Visible	24 February 1999	12.9–14.1	0.29/0.87	0.11/0.38	1100	0.04–0.12
Patches of Cb turret		14.1–15.3				
Minimum	24 February 1999		0.06	0.017	— ^b	—
Maximum	24 February 1999		0.75	0.074	— ^b	—
Cirrus	27 February 1999	15.3–15.8	≈ 0.25	≈ 0.035	1200 ^c	0.024

^aNote: These IWCs and the optical depth are obtained for particles with sizes between 0.7 and $25\ \mu\text{m}$ (i.e., the detection limits of the FSSP-300). The total ice water content as well as the optical depth of the cloud maybe much higher if larger particles are present.

^bFor these clouds, the geometrical thickness and also optical depth could not be estimated.

^cThe geometrical thicknesses of these clouds were estimated based upon the OLEX lidar measurements at 1064 nm (see Figure 11).

(near 17 km) into the lowermost stratosphere was executed during the outbound flight leg. The airplane was in the lower stratosphere during this leg from 11°S to 18°S. Then Geophysica performed a dip (i.e., an intermediate descent into and subsequent reascent from the troposphere) during which it turned around for its inbound flight. The return flight was along the same meridian at higher altitudes as can be seen in the right hand side of Figure 15. Figure 16 gives the vertical profiles of total water, ozone, N₂O, ambient temperature and particle number density of the entire flight. Between 17 and 21 km, above the tropopause, the particle number density increases. This is the lower part of the stratospheric Junge aerosol layer, the maximum of which may lie at higher altitudes, i.e., beyond the cruising altitude of Geophysica. The particle number concentrations measured during takeoff and landing at 5°S (Mahé) are similar to those encountered during the “dip” at 18°–19°S, if one considers the stratospheric data only in Figure 16. Thus these measurements do not indicate much of a geographic variation of the lower part of the Junge layer in this latitude band. This is supported by the particle size distributions shown in Figure 17. The size distributions are data averages over the flight segments labeled as “a,” “b,” “c,” and “d” in Figure 15. For the data reduction of the background aerosol measurements a refractive index of 1.44 was used in conjunction with Mie theory calculations, assuming these particles to be sulfuric acid droplets. Taking into account the statistical errors, these size distributions do not significantly differ in shape, but only in the absolute number densities. These considerations of the Junge layer aerosol have to be viewed with caution because only particles larger than 0.41 μm are detected by the FSSP-300 whereas the background layer contains smaller particles in larger numbers.

6. Conclusions

[32] Upper tropospheric clouds have been observed above the tropical Indian Ocean on 24 and 27 February 1999 during the APE-THESEO field campaign where the Russian high-altitude research aircraft “Geophysica” was used as measurement platform. These were ultrathin layers of subvisual cirrus at the tropopause, cloud patches near the Cb turret, and cirrus clouds in Cb anvil outflow regions. For the in situ aerosol size distribution measurements in the size range from approximately 0.5 to 23 μm a modified optical particle counter of the FSSP-300 type was utilized. Depolarization measurements by a microjoule lidar (MAL) resulted in values of 25–35% volume depolarization in visible clouds, ~4% in subvisual indicating that the cloud particles were slightly aspherical.

[33] The concurrent in situ total water measurements showed saturation with respect to ice directly above and below and supersaturation inside the analyzed clouds. Consequently for the data reduction of the FSSP-300 measurements the refractive index for ice was adopted.

[34] Table 1 provides a summary of the observed properties from the encountered clouds.

[35] The subvisual clouds at the tropopause with an air temperature of ~190 K occurred as ultrathin cloud layers with an horizontal extent of several 100 km. The geometrical thickness derived from lidar measurements was

in the range from below 100 m up to 400 m. The optical thickness was 0.0004–0.0005 for 632 nm wavelength, clearly within the range of values for subvisual clouds, while the particle concentration was 0.1–0.3 particles/cm³ (i.e., 100–300 L⁻¹) and 0.015 particles/cm³ (i.e., 15 L⁻¹) for sizes above 1 μm for these clouds. Based on the measured optical depths and geometrical thicknesses these cloud sheets belong to the geometrically and optically thinnest so far reported in the literature. In both cases, at the tropopause and in 13 km altitude, the size distribution of the subvisual clouds differs from the background aerosol only for particle sizes above 1 μm . For these larger particles the maximum in the size distribution is around 10 μm , which is in the range of earlier measurements and model calculations. In visible cirrus clouds the concentration of particles below 1 μm was significantly above the concentration of the background aerosol.

[36] On a flight with background aerosol conditions very little latitudinal variation of the aerosol concentration of the lower part of the Junge layer was observed in the lower stratosphere between 17 and 21 km in the latitude band from 5°S (Mahé) to 18°S.

[37] **Acknowledgments.** The authors would like to thank the pilots of Russian Geophysica and the German DLR Falcon for their enthusiasm and precision in the execution of the flights. We also thank Stefano Balestri (APE Srl., Italy), Thomas Peter (ETHZ, Switzerland), Ken Carslaw (University of Leeds, UK), and the whole “Geophysica community” including ground crews of both aircraft. The participation of the Forschungszentrum Jülich GmbH was supported by Gean national funding from BMBF under grant 01 LA 9829/3. The participation of the Observatory of Neuchâtel was supported by Swiss national funding OFES 97.0436 and FN R'Equip 21-53301-98. This research was financed by the Environment and Climate Program of the EU through contracts EV5V-CT93-0352 and ENV4-CT95-0143. Significant support was also provided by the Italian National Antarctic Research Program (PNRA), the University of Mainz, the Max-Planck Institute for Chemistry in Mainz, and the Forschungszentrum Jülich GmbH.

References

- Adriani, A., F. Cairo, M. Viterbini, S. Mandolini, L. Pulvirenti, and G. Di Donfrancesco, Multiwavelength aerosol scatterometer for airborne experiments to study the stratospheric particle optical properties, *J. Atmos. Oceanic Technol.*, 16, 1329–1336, 1999.
- Barnes, A. A., Observations of ice particles in clean air, *J. Rech. Atmos.*, 14, 311–315, 1980.
- Baumgardner, D., J. E. Dye, B. W. Gandrud, and R. G. Knollenberg, Interpretation of measurements made by the Forward Scattering Spectrometer Probe (FSSP-300) during the Airborne Arctic Stratospheric Expedition, *J. Geophys. Res.*, 97, 8035–8046, 1992.
- Boehm, M. T., J. Verlinde, and T. P. Ackerman, On the maintenance of high tropical cirrus, *J. Geophys. Res.*, 104, 24,423–24,433, 1999.
- Borrmann, S., S. Solomon, J. E. Dye, and B. Luo, The potential of cirrus clouds for heterogeneous chlorine activation, *Geophys. Res. Lett.*, 23, 2133–2136, 1996.
- Borrmann, S., B. Luo, and M. Mishchenko, The application of the T-matrix method to the measurement of aspherical ellipsoidal particles with forward scattering optical particle counters, *J. Aerosol Sci.*, 31, 789–799, 2000.
- Bregman, B., P.-H. Wang, and J. Lelieveld, Chemical ozone loss in the tropopause region on subvisible clouds, calculated with a chemistry-transport model, *J. Geophys. Res.*, 107(D3), doi:10.1029/2001JD000761, 2002.
- Cairo, F., G. Di Donfrancesco, A. Adriani, L. Pulvirenti, and F. Fierli, Comparison of various linear depolarization parameters measured by lidar, *Appl. Opt.*, 38, 4425–4432, 1999.
- Fahey, D. W., et al., In situ measurements constraining the role of sulphate aerosols in mid-latitude ozone depletion, *Nature*, 363, 509–514, 1993.
- Hamill, P., and G. Fiocco, Nitric acid aerosols at the tropical tropopause, *Geophys. Res. Lett.*, 15, 1189–1192, 1988.

- Heymsfield, A. J., Ice particles observed in a cirriform cloud at -83°C and implications for polar stratospheric clouds, *J. Atmos. Sci.*, **43**, 851–855, 1986.
- Heymsfield, A. J., and L. J. Jahnson, Microstructure of tropopause cirrus layers, in *Proc. Sixth Conf. on Aerospace and Aeronautical Meteorology*, pp. 43–48, Am. Meteorol. Soc., Boston, Mass., 1974.
- Heymsfield, A. J., and G. M. McFarquhar, High albedos of cirrus in the tropical Pacific warm pool: Microphysical interpretations from CEPEX and from Kwajalein, Marshall Island, *J. Atmos. Sci.*, **53**, 2424–2451, 1996.
- Jensen, E. J., O. B. Toon, H. B. Selkirk, J. D. Spinhirne, and M. R. Schoeberl, On the formation and persistence of subvisible cirrus clouds near the tropical tropopause, *J. Geophys. Res.*, **101**, 21,361–21,375, 1996a.
- Jensen, E. J., O. B. Toon, L. Pfister, and H. B. Selkirk, Dehydration of the upper troposphere and lower stratosphere by subvisible cirrus clouds near the tropical tropopause, *Geophys. Res. Lett.*, **23**, 825–828, 1996b.
- Jensen, E. J., W. G. Read, J. Mergenthaler, B. J. Sandor, L. Pfister, and A. Tabazadeh, High humidities and subvisible cirrus near the tropical tropopause, *Geophys. Res. Lett.*, **26**, 2347–2350, 1999.
- Keim, E. R., et al., Observations of large reductions in the NO/NO_y ratio near the mid-latitude tropopause and the role of heterogeneous chemistry, *Geophys. Res. Lett.*, **23**, 3223–3226, 1996.
- Knollenberg, R. G., A. J. Dascher, and D. Huffmann, Measurement of the aerosol and ice crystal populations in tropical stratospheric cumulonimbus anvils, *Geophys. Res. Lett.*, **9**, 613–616, 1982.
- Knollenberg, R. G., K. Kelly, and J. C. Wilson, Measurements of high number densities of ice crystals in the tops of tropical cumulonimbus, *J. Geophys. Res.*, **98**, 8639–8664, 1993.
- Kyrö, E., et al., Ozone measurements during the Airborne Polar Experiment: Aircraft instrument validation, isentropic trends, and hemispheric fields prior to the 1997 Arctic ozone depletion, *J. Geophys. Res.*, **105**, 14,599–14,611, 2000.
- Lynch, D. K., Subvisual cirrus: What it is and where you find it, *Proc. SPIE Int. Soc. Opt. Eng.*, **1934**, 264–274, 1993.
- Matthey, R., V. Mitev, G. Mileti, V. Makarov, A. Turin, M. Morandi, and V. Santacesaria, Miniature aerosol lidar for automated airborne application, in *Laser Radar Technology and Application V*, edited by G. Kamerman, *Proc. SPIE Int. Soc. Opt. Eng.*, **4035**, 44–53, 2000.
- McFarquhar, G. M., and A. J. Heymsfield, Microphysical characteristics of three anvils sampled during the Central Equatorial Pacific Experiment, *J. Atmos. Sci.*, **53**, 2401–2423, 1996.
- McFarquhar, G. M., A. J. Heymsfield, J. Spinhirne, and B. Hart, Thin and subvisual tropopause tropical cirrus: Observations and radiative impacts, *J. Atmos. Sci.*, **57**, 1841–1853, 2000.
- Omar, A. H., and C. S. Gardner, Observations by the Lidar In-Space Technology Experiment (LITE) of high-altitude cirrus clouds over the equator in regions exhibiting extremely cold temperatures, *J. Geophys. Res.*, **106**, 1227–1236, 2001.
- Prabhakara, C., R. S. Fraser, G. Dalu, M.-L. C. Wu, R. J. Curran, and T. Styles, Thin cirrus clouds: Seasonal distribution over oceans deduced from Nimbus-4 IRIS, *J. Appl. Meteorol.*, **27**, 379–399, 1988.
- Riediger, O., U. Schmidt, M. Strunk, and C. M. Volk, HAGAR: A new in-situ instrument for stratospheric balloons and high altitude aircraft, in *Stratospheric Ozone 1999, Proceedings of the Fifth European Symposium, Air Pollut. Res. Rep.*, vol. 73, edited by N. R. P. Harris et al., pp. 727–729, Eur. Comm., Brussels, 2000.
- Rosenfield, J. E., D. B. Considine, M. R. Schoeberl, and E. V. Browell, The impact of subvisible cirrus near the tropical tropopause on stratospheric water vapor, *Geophys. Res. Lett.*, **25**, 1883–1886, 1998.
- Santacesaria, V., et al., Clouds at the tropical tropopause: A case study during the APE-THESIO campaign over the western Indian Ocean, *J. Geophys. Res.*, doi:10.1029/2002JD002166, in press, 2002.
- Sassen, K., and B. S. Cho, Subvisual-thin cirrus lidar dataset for satellite verification and climatological research, *J. Appl. Meteorol.*, **31**, 1275–1285, 1992.
- Sassen, K., M. K. Griffin, and G. C. Dodd, Optical scattering and microphysical properties of subvisual cirrus clouds and climatic implications, *J. Appl. Meteorol.*, **28**, 91–98, 1989.
- Schmidt, E. O., and D. K. Lynch, Subvisual cirrus: Associations to the dynamic atmosphere and radiative effects, *Proc. SPIE Int. Soc. Opt. Eng.*, **2578**, 68–75, 1995.
- Schmidt, E. O., J. M. Alvarez, M. A. Vaughan, and D. P. Wylie, A review of subvisual cirrus morphology, *Proc. SPIE Int. Soc. Opt. Eng.*, **1934**, 230–239, 1993.
- Solomon, S., S. Borrmann, R. R. Garcia, R. Portmann, L. Thomason, L. R. Poole, D. Winker, and M. P. McCormick, Heterogeneous chlorine chemistry in the tropopause region, *J. Geophys. Res.*, **102**, 21,411–21,429, 1997.
- Stefanutti, L., L. Sokolov, S. Balestri, A. R. MacKenzie, and V. Khatatov, The M-55 Geophysica as platform for the Airborne Polar Experiment, *J. Atmos. Oceanic Technol.*, **16**, 1303–1312, 1999.
- Ström, J., B. Strauss, T. Anderson, F. Schröder, J. Heintzenberg, and P. Wendling, In situ observations of the microphysical properties of young cirrus clouds, *J. Atmos. Sci.*, **54**, 2542–2553, 1997.
- Uthe, E. E. and P. B. Russell, Lidar observations of tropical high altitude cirrus clouds, in *Proceedings of the IAMAP Symposium on Radiation in the Atmosphere, Garmisch-Partenkirchen, Germany, 19–28 August 1976*, edited by H. J. Bolle, pp. 242–244, Science, Enfield, N.H., 1977.
- Wang, P.-H., P. Minnis, M. P. McCormick, G. S. Kent, and K. M. Skeens, A 6-year climatology of cloud occurrence frequency from Stratospheric Aerosol and Gas Experiment II observations (1985–1990), *J. Geophys. Res.*, **101**, 29,407–29,429, 1996.
- Winker, D. M., and C. R. Trepte, Laminar cirrus observed near the tropical tropopause by LITE, *Geophys. Res. Lett.*, **25**, 3351–3354, 1998.
- Wirth, M., and W. Renger, Evidence of large scale ozone depletion within the arctic polar vortex 94/95 based on airborne LIDAR measurements, *Geophys. Res. Lett.*, **23**, 813–816, 1996.
- Zöger, M., et al., FISH: A novel family of balloonborne and airborne Lyman- α photofragment fluorescence hygrometers, *J. Geophys. Res.*, **104**, 1807–1816, 1999.

J. Beuermann, Institut für Chemie und Dynamik der Geosphäre (ICG-1), Forschungszentrum Jülich GmbH, Jülich, Germany.

S. Borrmann and A. Thomas, Institut für Physik der Atmosphäre, Universität Mainz, Mainz, Germany. (borrmann@uni-mainz.de)

F. Cairo, Istituto di Scienze dell'Atmosfera e del Clima, CNR, Rome, Italy.

C. Kiemle, Institut für Physik der Atmosphäre, DLR, Oberpfaffenhofen, Germany.

B. Lepuchov, Myasishchev Design Bureau, Moscow, Russia.

A. R. MacKenzie, Environmental Science Department, Lancaster University, Lancaster, UK.

R. Matthey, Observatoire Cantonal, Neuchâtel, Switzerland.

V. Rudakov and V. Yushkov, Central Aerological Observatory, Moscow, Russia.

V. Santacesaria and L. Stefanutti, Istituto di Ricerca sulle Onde Elettromagnetiche, CNR, Florence, Italy.

M. Volk, Institut für Meteorologie und Geophysik, Universität Frankfurt, Frankfurt, Germany.